Near-shore wind resource estimation using lidar measurements and modelling

Floors, Rogier Ralph; Hahmann, Andrea N.; Pena Diaz, Alfredo

Publication date:
2017

Document Version
Publisher's PDF, also known as Version of record

Citation (APA):
Floors, R. R., Hahmann, A. N., & Pena Diaz, A. (2017). Near-shore wind resource estimation using lidar measurements and modelling. Poster session presented at WindEurope Offshore 2017, London, United Kingdom.

PO.026

Near-shore wind resource estimation using lidar measurements and modelling

Rogier Floors, Andrea N. Hahmann and Alfredo Peña
DTU Wind Energy

Abstract

The atmospheric flow in the coastal zone is investigated using (scanning) lidars, mast measurements and the mesoscale WRF model. The WRF model is set-up in 12 different configurations using 2 planetary boundary-layer schemes, 3 horizontal grid spacings and varied sources of land use, and initial and lower boundary conditions.

Objectives

- Describe the impact of boundary layer scheme, resolution, land use data and atmospheric forcing on the WRF modelled wind speed
- Estimate the wind resource using scanning and vertically profiling lidars

Methods

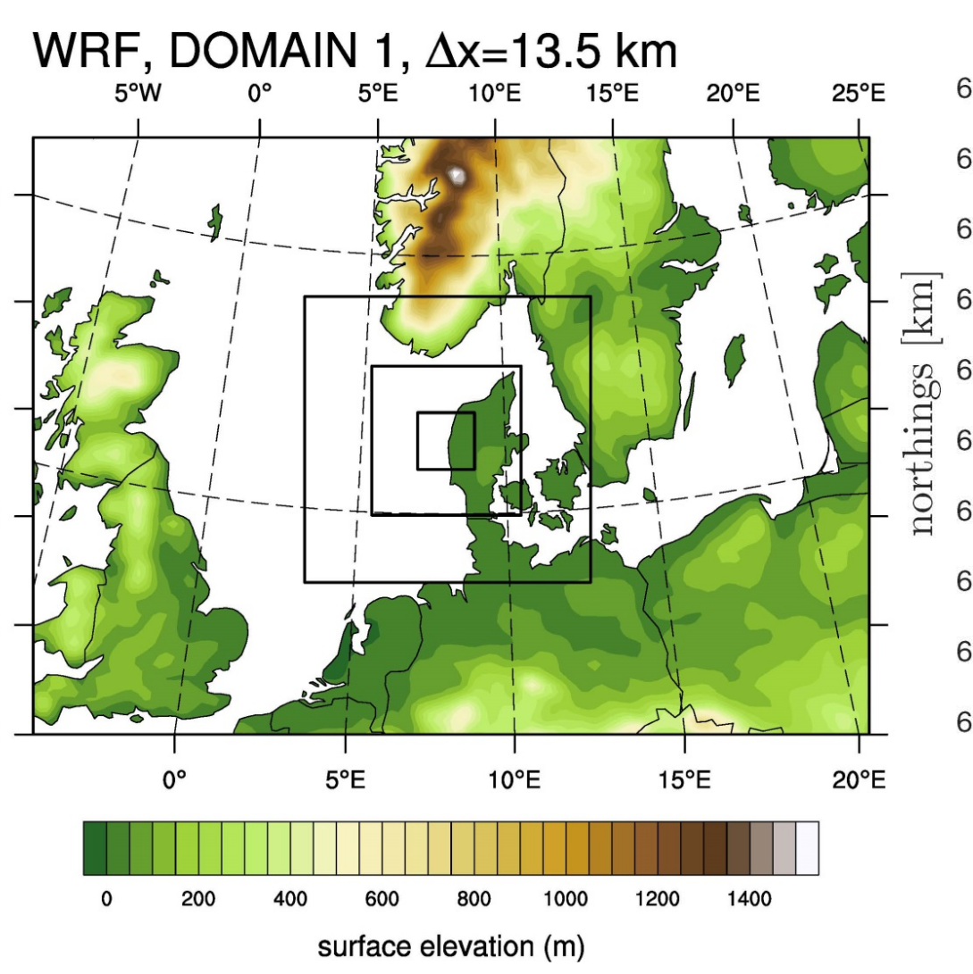

The WRF model was set up to cover northwestern Europe.

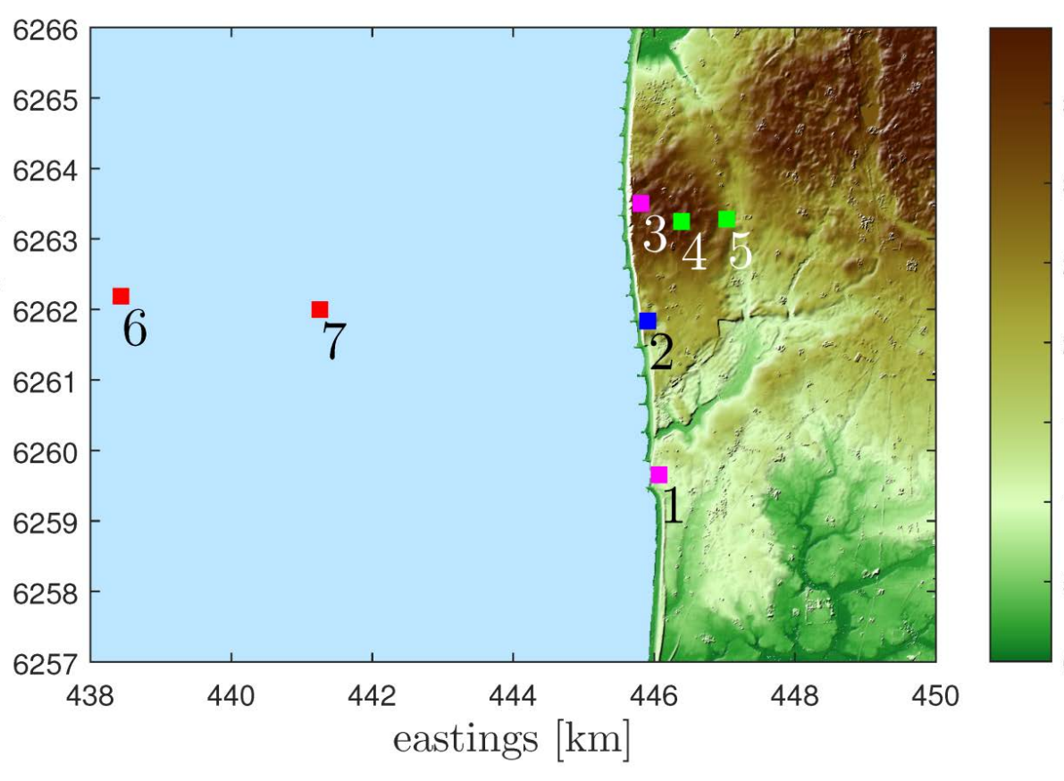

The scanning lidars were located in pos 1-3, vertically profiling lidars in pos. 2, 4-5 and floating lidars in pos . 6 and 7 (see below).

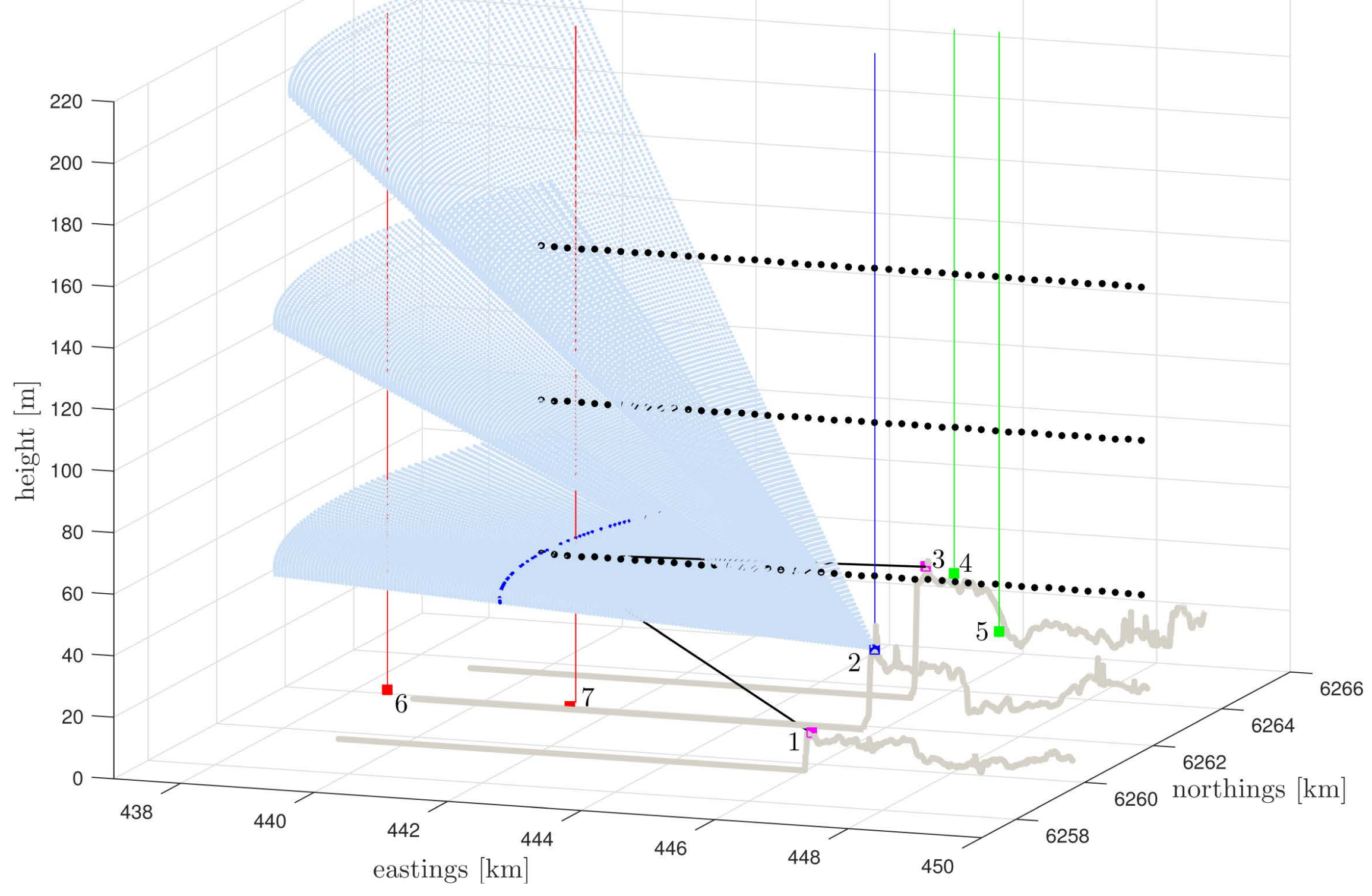

Overview of the scanning patterns during the RUNE campaign. The light blue points denote the sector scan, the black dots denote the collocated range gates from the synchronized scanning lidars, the green and blue lines denote the vertically profiling lidars, the red line denotes the lidar buoy and the dark blue points from the sector scan denote an arc from which the wind vector can be reconstructed.

Model set-ups

All model setups were run from the 1 Nov 2015 to 1 Mar 2016 using the WRF model, version 3.6, using 70 vertical levels with the model top at 50 hPa; The first 10 levels are located approximately at: 5.6, 17.4, 29.7, 42.7, 56.5, 71.0, 86.3, 102.5, 119.7 and 137.8 m.

Model Simulation	Atmos. Bound. cond.	PBL scheme	SST source	land cover source	horizontal grid spacing [m]
YSU_2	FNL	YSU	DMI	CORINE	2000
YSU_1	FNL	YSU	DMI	CORINE	1000
$\mathrm{YSU}_{0.5}$	FNL	YSU	DMI	CORINE	500
MYJ_2	FNL	MYJ	DMI	CORINE	2000
MYJ_1	FNL	MYJ	DMI	CORINE	1000
$\mathrm{MYJ}_{0.5}$	FNL	MYJ	DMI	CORINE	500
$\mathrm{YSU}_{\mathrm{HRSST}}$	FNL	YSU	HR	CORINE	2000
$\mathrm{MYJ}_{\mathrm{HRSST}}$	FNL	MYJ	HR	CORINE	2000
$\mathrm{YSU}_{\mathrm{USGS}}$	FNL	YSU	DMI	USGS	2000
$\mathrm{MYJ}_{\mathrm{USGS}}$	FNL	MYJ	DMI	USGS	2000
$\mathrm{YSU}_{\mathrm{ERA}}$	ERA	YSU	DMI	CORINE	2000
$\mathrm{MYJ}_{\mathrm{ERA}}$	ERA	MYJ	DMI	CORINE	2000

Horizontal transects

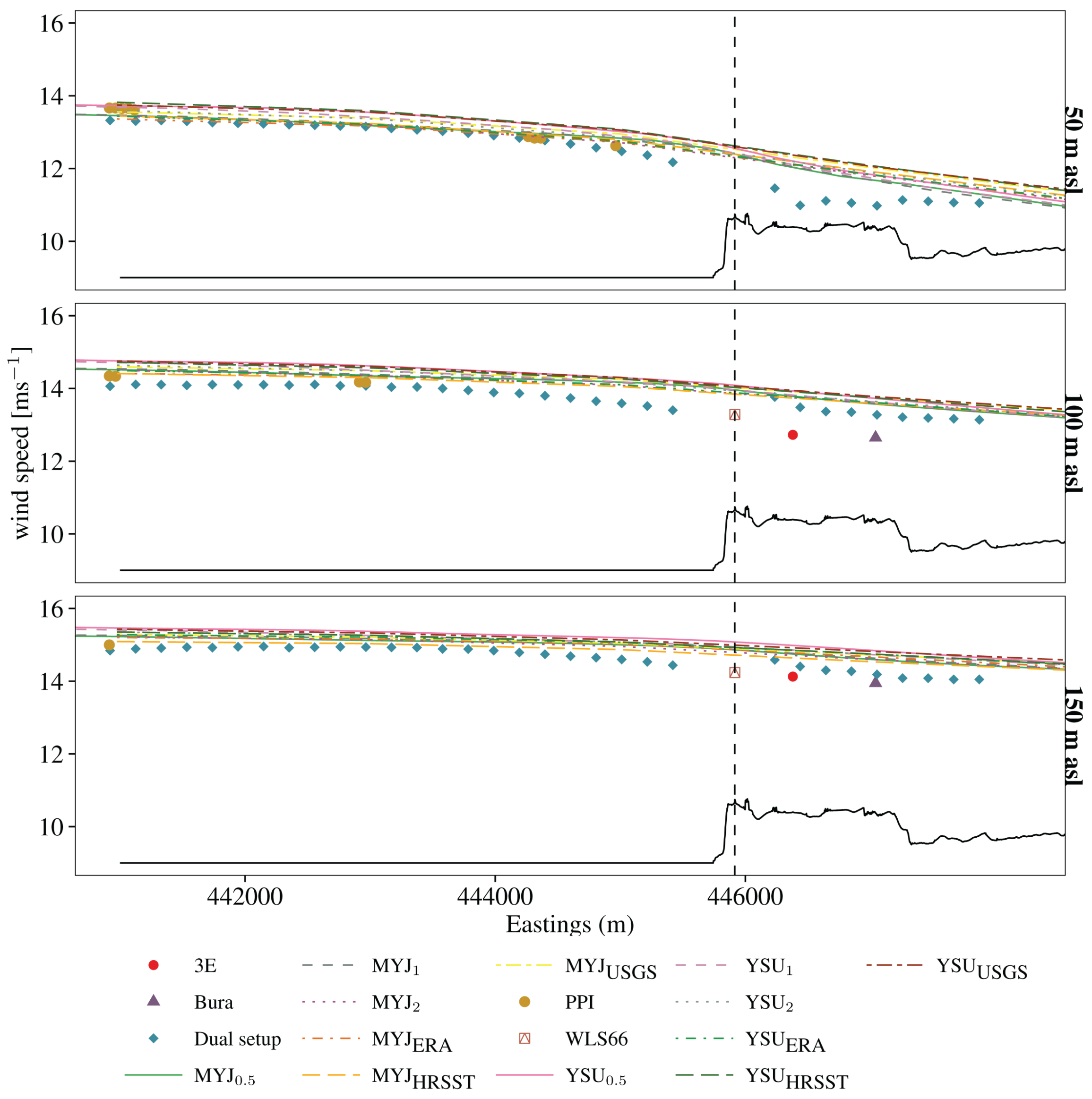

The horizontal gradient in mean winds speed across the experimental site from 5 km offshore up to 2 km inland is shown above. Data were filtered based on the CNR ratio (measurement quality) and availability in the whole transect, leaving 731 transects at 50, 100 and 150 m. The model output from all simulations was extracted during the same 10-min intervals.

Generally the model prediction show slightly higher wind speeds offshore. Over land at 50 m the observed wind speed is much lower than the modelled wind . The WRF model cannot capture the effect of the cliff well, partly due to its coarser resolution.

Both scanning lidar systems agree well far offshore. The vertical profiling lidars show a lower mean wind speed.

Vertical profiles

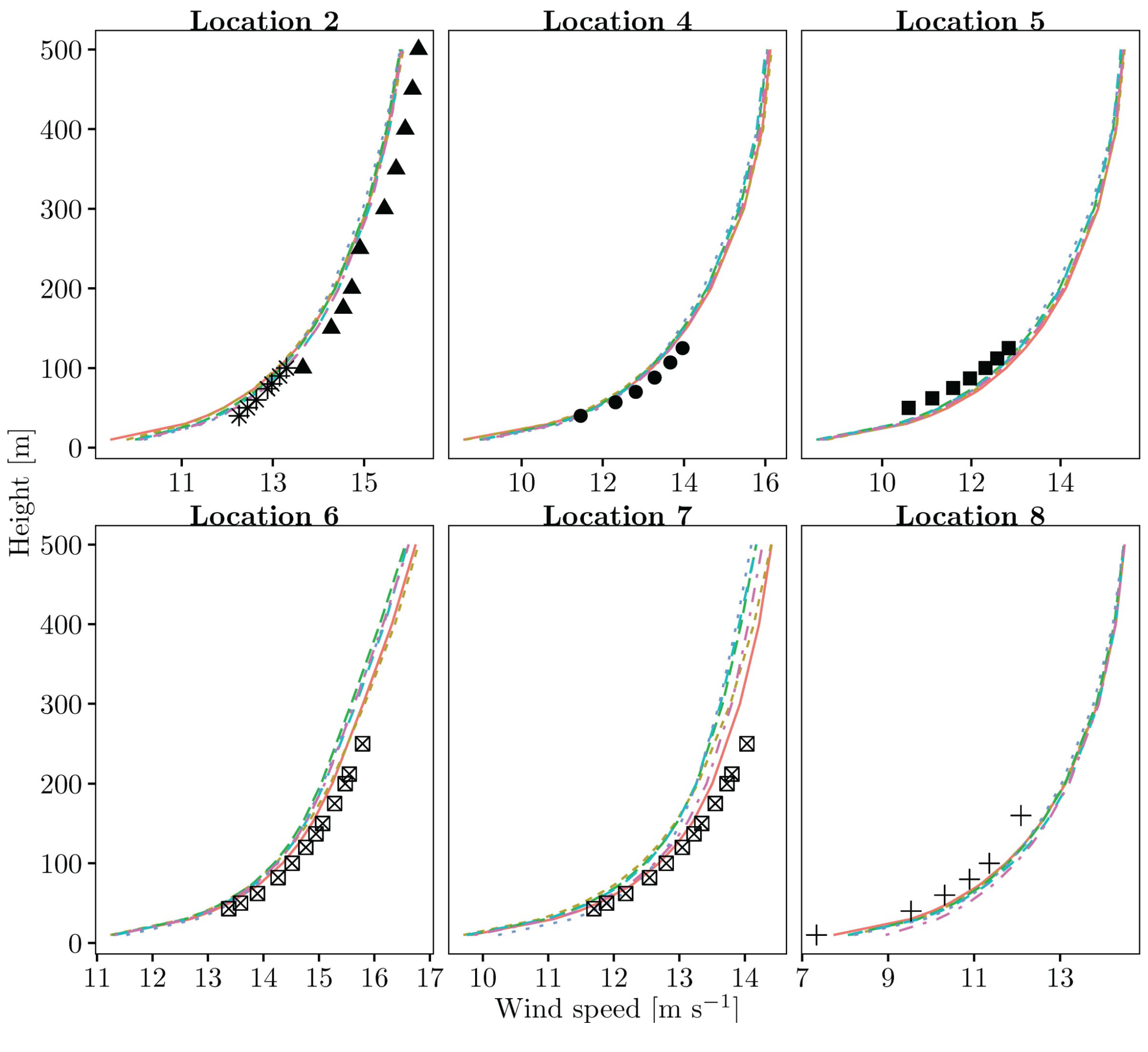

Mean vertical wind speed profiles at 6 different locations (see map at the left) observed by lidars and modelled with the MYJ scheme (abbreviations explained to the left).

In the figure above it can be seen that shape of the wind profile is modelled well by all model simulations and than the bias is generally less than 0.5 m/s. Note the different scale at the x-axis: the wind speed at the inland locations is much lower than at offshore locations close to the ground. At location two, two lidars were measuring at the same location and both of them are shown.

Velocity spectra and error metrics

Velocity spectra are often used to gain insight in the ability of models or observations to represent atmospheric motions. Below the spectral energy from the cup anemometer at 100 m at the Høvsøre mast is shown as a function of frequency. At low frequencies (left) the model and observations compare well, showing the model resolves the energy at these scales. At high frequencies, the model set-ups with fine horizontal grid spacing have more energy than the observations. This has an impact on the model performance (see below).

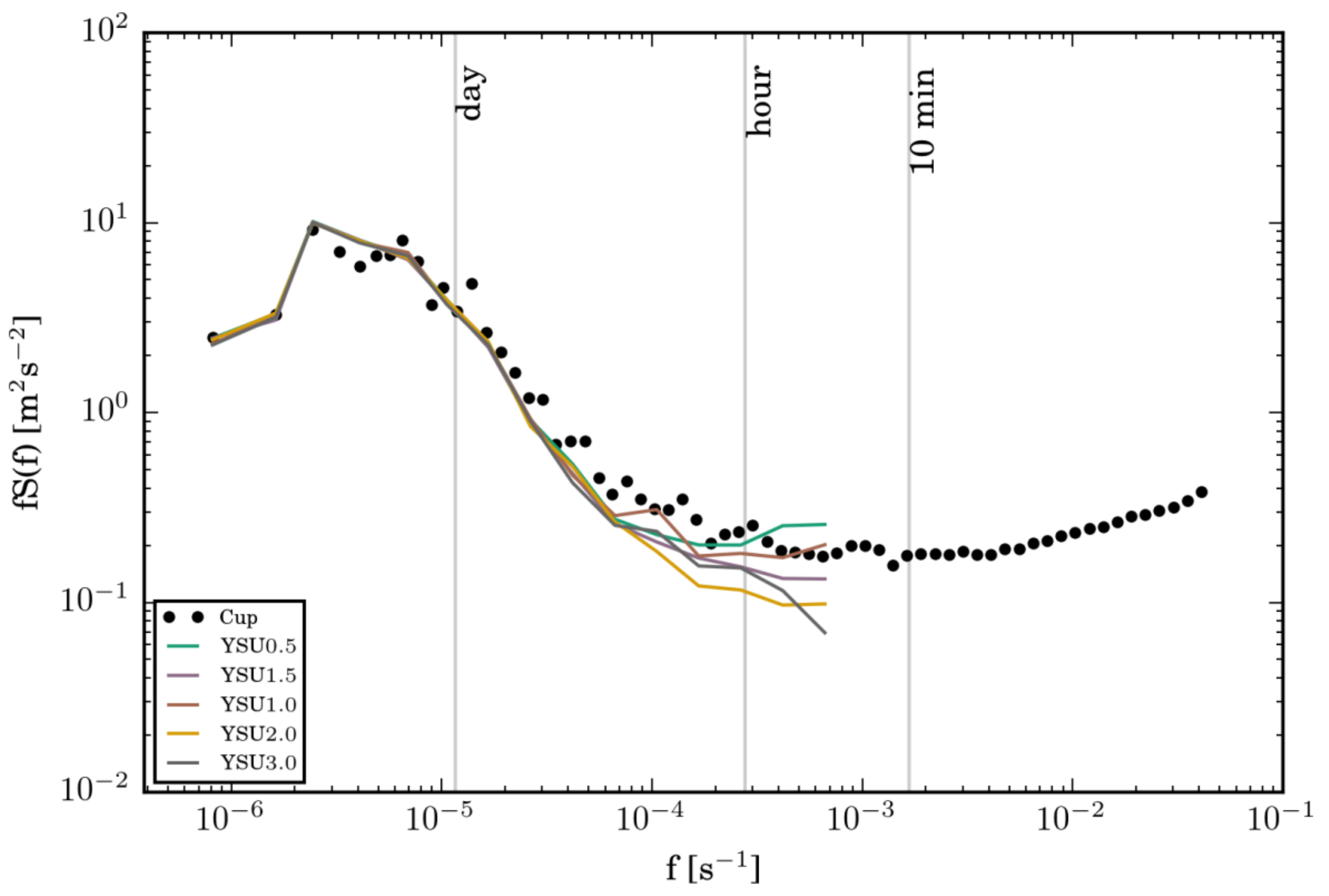

The table below shows a summary of different metrics during the whole campaign for all sites, for example the root-mean-square error (RMSE) and Pearson correlation coefficient (R). There were 237493 10-minute mean measurements available. The simulations with the MYJ scheme and the ERA-interim boundary conditions have the lowest RMSE and mean absolute error. It can be seen that using a higher resolution leads to worse error metrics.

Setup	RMSE ($\mathrm{m\,s^{-1}}$)	Mean abs. err. ($\mathrm{m\,s^{-1}}$)	Mean bias ($\mathrm{m\,s^{-1}}$)	R (-)	Mean mod. ($\mathrm{m\,s^{-1}}$)	Mean obs. ($\mathrm{m\,s^{-1}}$)	Mean rel. err. (%)
$\mathrm{MYJ}_{0.5}$	2.15	1.56	-0.16	0.93	12.11	12.27	-1.31
MYJ_1	2.23	1.61	-0.16	0.92	12.11	12.27	-1.29
MYJ_2	2.07	1.50	-0.10	0.93	12.17	12.27	-0.79
$\mathrm{MYJ}_{\mathrm{ERA}}$	**1.96**	**1.48**	-0.04	**0.94**	12.23	12.27	-0.31
$\mathrm{MYJ}_{\mathrm{HRSST}}$	2.07	1.51	-0.05	0.93	12.22	12.27	-0.39
$\mathrm{MYJ}_{\mathrm{USGS}}$	2.11	1.56	0.09	0.93	12.36	12.27	0.73
$\mathrm{YSU}_{0.5}$	2.28	1.65	-0.09	0.92	12.17	12.27	-0.76
YSU_1	2.33	1.67	-0.16	0.92	12.11	12.27	-1.31
YSU_2	2.18	1.57	**0.02**	0.93	12.29	12.27	**0.15**
$\mathrm{YSU}_{\mathrm{ERA}}$	2.07	1.54	0.06	0.93	12.33	12.27	0.47
$\mathrm{YSU}_{\mathrm{HRSST}}$	2.14	1.54	0.14	0.93	12.41	12.27	1.14
$\mathrm{YSU}_{\mathrm{USGS}}$	2.24	1.64	0.20	0.92	12.47	12.27	1.61

Conclusions

The WRF modelled wind speed was close to scanning lidar observations in a transect across the coastline, although all simulations showed wind speeds that were slightly higher than observed. Inland at 50 m, the model did not capture the strong decrease in mean wind speed resulting from the surface roughness change when moving eastward from the coastline. Using ERA-interim data as boundary conditions improved the model skill scores. Using a finer horizontal grid spacing deteriorated the model performance. Modelled and observed spectra were compared and showed that the horizontal grid spacing had a large impact on the ability of the different setups to capture high frequency atmospheric motions. Combining the WRF model with lidar measurements can be useful to describe and understand the flow in the coastal zone.

References

Floors, R., A.N Hahmann and A. Peña, 2017, Sensitivity study of the WRF model to simulate the flow in the coastal zone *Quartely Journal of the Royal Meteorological Society* (in prep.)

Floors, R; Hahmann, A. N.; Peña, A.; Karagali, I., 2016, Estimating near-shore wind resources. *DTU Wind Energy*, 49 p. (DTU Wind Energy E; No. 0116).

Floors, R; Lea, G.; Peña, A; Karagali, I.; Ahsbahs, T., 2016 Report on RUNE's coastal experiment and first inter-comparisons between measurements systems. *DTU Wind Energy*,. 33 p. (DTU Wind Energy E; No. 0115).

Lea, G.; Courtney, M., 2016, Validation of long-range scanning lidars deployed around the Høvsøre Test Station. *DTU Wind Energy*, 2016. 19 p. (DTU Wind Energy E; No. 0114).

The RUNE Experiment—A Database of Remote-Sensing Observations of Near-Shore Winds. Floors, R.; Peña, A.; Lea, G.; Vasiljevic, N.; Simon, E.; Courtney, M. *Remote Sensing*, Vol. 8, No. 11, 2016. http://www.mdpi.com/2072-4292/8/11/884

Offshore WIND ENERGY 2017
LONDON 6-8 JUNE
Co-organised by:
Wind EUROPE
renewableUK

offshorewind2017.com
#offshore2017